

Influence of Spacing of Multiple Impellers on Power Input in an Industrial-Scale Aerated Stirred Tank Reactor

Jürgen Fitschen^{1,*}, Marc Maly¹, Annika Rosseburg¹, Johannes Wutz², Thomas Wucherpennig², and Michael Schlüter¹

DOI: 10.1002/cite.201900121

 This is an open access article under the terms of the Creative Commons Attribution-NonCommercial License, which permits use, distribution and reproduction in any medium, provided the original work is properly cited and is not used for commercial purposes.

Despite the fact that aerated stirred tank reactors are widely used in industry and often studied, their design and scale-up still remains challenging. Especially the specific power input is a crucial and geometry-dependent scale-up parameter, usually calculated with the dimensionless power number Po . Within the scope of this study, the power number is measured for different stirrer types and configurations in a laboratory and an industrial-scale aerated stirred tank reactor. Good agreements to literature are found for the unaerated case for the two-stage stirrer configurations at different stirrer spacing for both scales. By literature only the aerated case in the laboratory scale can be predicted. Scale-up of an aerated industrial-scale reactor is challenging because of a specific influence of the aeration. In case of a three-stage Rushton configuration, an asymmetrical distribution of the stirrers should be preferred to ensure a high power number as well as good power performance under aerated conditions.

Keywords: Aerated stirred tank reactors, Power input performance, Scale-up

Received: August 27, 2019; *revised:* November 04, 2019; *accepted:* November 05, 2019

1 Introduction

Due to their simple operating mode, low investment costs and flexibility, aerated stirred tank reactors are still used widely in industries connected to chemical and biochemical engineering today. Important parameters and challenges for a variety of applications in these different fields are efficient mixing of two-phase flows with high heat- and mass transfer performance, short mixing times, and an efficient energy input [1]. Because of their significance, these parameters have been investigated intensively in the past decades. The findings have been used to enhance modeling and simulation of processes in these apparatuses. An important task here is the scale-up of processes from small laboratory-scale reactors with few liters in volume to the dimensions commonly found in industrial applications with several cubic meters.

Despite the undertaken research, the design and scale-up still presents an immense challenge as the large variety of influencing parameters makes this task an ambitious one. This is already clear from the fact that different scale-up procedures exist. In general, geometric relations should be kept constant when transferring a process from lab to industrial scale. Additionally, to ensure constant volumetric mass transfer values, it is recommended to keep the volumetric power input as well as the superficial gas velocity constant. Other scale-up approaches are based on, e.g., constant shear rate, impeller tip speed or constant mixing per-

formance [2–5]. First investigations in this field were focused on mixing time, global flow structures and gas hold-up (e.g., [6–11]), but over the years, the focus shifted from global measurements to more local experimental analysis. This shift was accompanied by a greater interest in bubble size distributions [12, 13], local gas hold-up [11, 14, 15] and liquid and gas velocities [16, 17]. However, reliable design and scale-up remains a challenging task.

Therefore, a large-scale acrylic glass reactor with a total volume of $V_R = 15 \text{ m}^3$ and total optical access has been erected at Hamburg University of Technology together with Boehringer Ingelheim Pharma GmbH & Co. KG to expand available data on large-scale reactors. The objective of this project is to enable a more reliable modeling and scale-up as well as transfer between different systems. As part of these investigations, several measurement techniques are used for the different investigated phenomena like optical

¹Jürgen Fitschen, Marc Maly, Annika Rosseburg, Prof. Dr.-Ing. Michael Schlüter
juergen.fitschen@tuhh.de

Hamburg University of Technology, Institute of Multiphase Flows, Eißendorfer Straße 38, 21073 Hamburg, Germany.

²Johannes Wutz, Dr. Thomas Wucherpennig
Boehringer Ingelheim Pharma GmbH & Co. KG, Late Stage USP Development, Bioprocess Development Biologicals, Birkendorfer Strasse 65, 88397 Biberach an der Riss, Germany.

measurement techniques to determine the mixing time [18], endoscopic optical probes to measure bubble size distributions or inline oxygen and carbon dioxide sensors to measure volumetric mass transfer coefficients. This article presents the study on the influence of spacing of multiple impellers on power input in an industrial-scale aerated stirred tank reactor.

2 Theory

In case of scaling up pharmaceutical cultivation processes, the volumetric power input is a crucial key parameter. For instance, the shear rates introduced by the stirrer increase with increasing power input, which may lead to cell damage or death of the cell if critical shear rates are exceeded [19]. This often results in lower power input for animal cell culture processes [20]. The power input is defined as

$$P = 2\pi Mn \quad (1)$$

where M is the torque at the stirrer shaft and n the stirrer frequency. If the torque is measured behind the shaft bearing, the bearing idling torque must be taken into account.

Besides the power input introduced by the stirrer, aeration is an important factor for the hydrodynamic behavior and shear stress. The power input P_G in the aerated case is compared to the input P_0 in the unaerated case. The ratio P_G/P_0 is reported as a function of the stirrer frequency for a given gas flow rate. The decrease in power consumption (compared to the unaerated system) is dependent on the setup of impellers used, e.g., the usage of different combina-

tions of impellers with a predominantly axial or radial configuration, where axial configurations reportedly have a better hydraulic efficiency [21].

Various correlations exist in literature to calculate and predict the ratio of power input P_G during aeration to the power input P_0 of the unaerated system. A selection of correlations can be found in Tab. 1. Due to the number of different impellers available on the market and the complexity of the hydrodynamics of different systems, literature data are often insufficient for the task of designing and controlling gas-liquid stirred reactors [21].

Different approaches for the design of systems are suggested by Vogel [27], which are based on, e.g., mixing time, impeller tip speed or specific power input. Of these, the specific power input criterion is probably the most accepted one for scale-up and process transfer between bioreactors [28]. Due to the wide variety of geometries, correlations in literature are almost exclusively applicable for a specific studied vessel; the more a system deviates from this vessel, the less applicable the correlations are [28]. Important factors here are the geometries of the vessel and the impellers, impeller spacing and the effect of aeration on power input [28]. For comparison of the impeller performance of different systems and in scale up, a nondimensional method using the power number Po and Reynolds number Re is employed since the relationship between these two numbers normalizes the power input to the characteristics of an impeller [29]. The power number is defined as

$$Po = \frac{P}{\rho n^3 d^5} \quad (2)$$

Table 1. Selection of correlations for the ratio of P_G/P_0 .

Correlation	Ref.	Remarks
$\frac{P_G}{P_0} = 1 - 12.6Fl_G, Fl_G < 0.035$	(10) [22]	$Fl_G = \frac{q_G}{n d^3}$ (11)
$\frac{P_G}{P_0} = 0.62 - 1.85Fl_G, Fl_G < 0.035$	(12)	
$\log\left(\frac{P_G}{P_0}\right) = -192\left(\frac{d}{D}\right)^{4.38} \left(\frac{\rho d^2 n}{\eta}\right)^{0.115} Fr^{1.96} \left(\frac{d}{v}\right) Fl$	(13) [23]	$Fr = \frac{n^2 d}{g}$ (14)
		$Fl = \frac{q}{nd^3}$ (15)
$\frac{P_G}{P_0} = 0.497\left(\frac{q_G}{nd^3}\right)^{-0.38} \left(\frac{\rho d^3 n^2}{\sigma}\right)^{-0.18}$	(16) [24]	
$\frac{P_G}{P_0} = 0.0312Fr^{-0.16} Re^{0.064} Fl^{-0.38} \left(\frac{d}{D}\right)^{0.8}$	(17) [25]	$V \leq 30 m^3; 1.8 < D/d < 3.7$
$\frac{P_G}{P_0} = 0.1\left(\frac{q_G}{nV}\right)^{-0.25} \left(\frac{n^2 d^4}{gWV^{2/3}}\right)^{-0.2}$	(18) [26]	$V \leq 51 m^3; u_G \leq 0.053 m s^{-1}$

where P is the power input, ρ the fluid density, n the stirrer frequency and d the stirrer diameter. The power input

$$P = 2n\pi M_{\text{stirrer}} \quad (3)$$

is defined by the stirrer frequency n and the stirrer torque M_{stirrer} . While the stirrer Reynolds number

$$Re = \frac{\rho n d^2}{\eta} \quad (4)$$

is defined by the dynamic viscosity η . It is used to describe the hydrodynamic behavior. The power number is reportedly not affected by spacing of the stirrers in unbaffled systems [30, 31].

Gas-liquid reactors equipped with multiple impellers ensure a higher efficiency of gas utilization and a longer retention time [21]. In these setups, a variety of traditional radial turbines and axial impellers can be found. An even dispersion of gas in liquid, a good mass transfer performance and low energy consumption are desired properties of these impellers and their combinations [21].

With sufficient clearance between the impellers, avoiding any interaction between them, the total power input in an unaerated system was found to be the sum of the power consumption of the individual impellers [21, 32]. The ratio of the diameter d of the impeller to the diameter D of the tank should be between 0.3 and 0.5, approximately 0.3 for radial flow impellers. Impellers that are too small do not generate enough fluid movement; oversized impellers require more power while being less efficient [27]. Spacing between impellers is important, as large spacing leads to insufficient mixing, while spacing that is too small decreases the power imparted to the fluid by up to 35% compared to properly spaced setups [33, 35]. Reportedly, spacing between impellers should range between 1.0 and $2.0d$, while the bottom clearance should be $1.0d$. The adequate number N of impellers can, thus, be derived from

$$\frac{H_L - d}{d} > N > \frac{H_L - 2d}{2d} \quad (5)$$

where H_L is the height of liquid in the reactor [37]. Independent behavior of impellers has been reported for pitched blade turbines in tap water as starting with a spacing of $1.55d$, while for two Rushton turbines it has been reported to start at a greater spacing of $1.65d$ [30, 31, 34]. For small gas flow rates, a sharp increase in Po is reported for dual Rushton turbines for spacing in the range of 0.6 to $0.8d$, which is much smaller for higher gas flow rates [34]. For a dual pitched blade configuration, the effect of impeller spacing on power consumption is reportedly smaller in the flooded regime than for a dual Rushton configuration. However, a dual pitched blade configuration already starts acting independently at a spacing of $0.45d$ for high gas flow rates [34].

The literature survey shows that a variety of studies on the power input as well as hydrodynamic characteristics of single and multistage stirrer setups has already been done. Besides that, most data have been measured on small-scale reactors.



Figure 1. Photo of the acrylic glass reactor at the Institute of Multiphase Flows [18].

3 Experimental Setup and Measurement Procedure

Experiments are carried out in an industrial-scale acrylic glass reactor (see Fig. 1) and are compared to a 30-L twin with a diameter $D = 2$ m and 0.288 m and a total volume $V_R = 15$ m³ and 0.03 m³, respectively. Three baffles of width $L_B = D/10$ and a distance of 120° are mounted at the reactor wall. The only difference between both reactors is the agitator; while the industrial reactor is equipped with a bottom-mounted magnetic agitator (Zeta BMRF prototype), the lab-scale reactor is equipped with a top-mounted agitator.

During the investigations, up to three turbines ($d/D = 0.33$) are used. The spacing s (see Fig. 2) between these impellers is varied and clearance to the bottom of the reactor is kept constant for different measurements. Aeration of the system is achieved by use of an open tube sparger, which is located below the impellers. A torque measuring cell is installed at the stirrer shaft (industrial reactor: Lorenz DR-3000; lab-scale reactor: HiTec Zang ViscoPakt Rheo X7) to precisely measure the induced torque by the impeller. An MFC (Bronkhorst EL-Flow) is used to control the gas flow rate. Two thermocouple type K temperature probes monitor the temperature within the reactor. An external heat exchanger is used to keep the temperature level

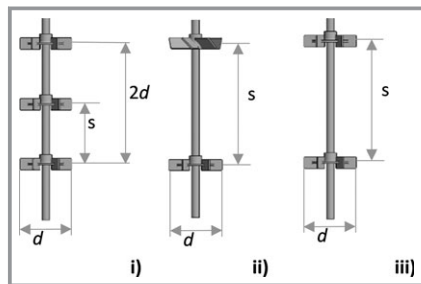


Figure 2. Visualization of the spacing for the three different stirrer configurations, three-stage Rushton (i), Rushton+pitched blade (ii) and two-stage Rushton (iii).

within the reactor constant. This external loop is switched off during the measurements. Due to the lid of the reactor and the good isolation characteristics of the acrylic glass, the temperature loss is about 0.1 K h^{-1} and, therefore, adiabatic conditions can be assumed.

For a given set of stirrer geometries and spacing between the stirrers, the momentum on the stirrer shaft is measured in operation over a wide range of different stirrer frequencies. An overview of the geometries used is given in Tab. 2. The pitch of the pitched blade is 45° .

Furthermore, the measurements are undertaken under aerated conditions for three different gassing rates, as well as in unaerated conditions. With knowledge of the idling torque and the parameters of the stirrer, the recorded momentum can be used to calculate the energy input for the different investigated sets of spacing and aeration parameters according to Eq. (1).

4 Experimental Results

The following part provides the experimental results of the power input measurements in a 30-L and 15 000-L unaerated stirred tank reactor. First, the evaluation of the torque measurements will be described exemplarily, followed by the results for the unaerated system. Finally, the results for the aerated system will be presented.

For design reasons, the torque sensor is mounted between the electrical motor and the shaft bearing. Therefore, the measured torque

$$M_{\text{total}} = M_{\text{bearing}} + M_{\text{stirrer}} \quad (6)$$

is the sum of the torque resulting from the bearing and the stirrer. To determine the power number Po , the torque from the bearing (4–12 Nm from 20 to 80 rpm) has to be subtracted from the total torque M_{total} . The determined stirrer torque is exemplarily plotted in Fig. 3 over the squared stirrer frequency. Here it can be stated that the torque

$$M_{\text{stirrer}} = a n^2 + b \quad (7)$$

can be fitted with a quality of $r^2 = 1$. The deviation from the origin of the fitted curve can be explained by an overall measurement offset of the torque measurement system and has to be subtracted from the measured torque. Therefore, only the slope a of the fitted curve will be used to calculate the unaerated power number

$$Po = \frac{2\pi Mn}{\rho n^3 d^5} = \frac{2\pi(a n^2)n}{\rho n^3 d^5} = \frac{2\pi a}{\rho d^5} \quad (8)$$

The determined unaerated power numbers Po for the given parameters in Tab. 2 are shown in Fig. 4. It is noticeable that the power number in the 30-L system is always smaller compared to the industrial scale. This is mainly due to the fact that the industrial-scale reactor is equipped with a bottom-driven magnetic stirrer with a broad support structure whereas the 30-L scale reactor is agitated from the top.

Therefore, the normalized power number

$$Po_{\text{norm}} = \frac{Po_i}{Po_{\text{Rt},i}} \quad (9)$$

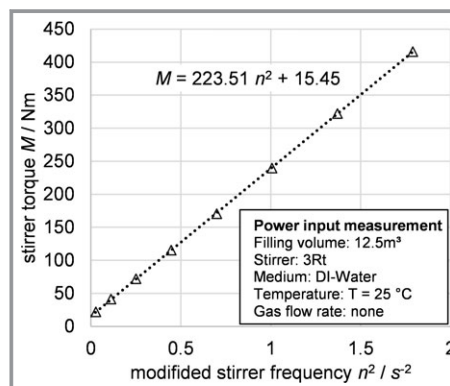


Figure 3. Stirrer torque M plotted over modified stirrer frequency n^2 to determine the influence of the measurement offset error.

Table 2. Overview of test parameters and geometries for the 30-L and 15 000-L scale; *outer stirrers fixed at positions $s/d = 0$ and 2.

Setup	Stirrer setup	Dimensionless stirrer pitch s/d [-]	Superficial gas flow rate u_G [mm s^{-1}]	Stirrer frequency n [rpm]		Reynolds number Re [-]		Reactor volume V [m^3]
				30 L	15 000 L	30 L	15 000 L	
a	Rushton + pitched blade (RtPb)	0.25–2.5	1.06–2.12	–	20–80	–	147 408–589 633	12.5
b	2x Rushton (2Rt)	0.25–2.5	1.06–2.12	100–400	20–80	15360–61400	147 408–589 633	0.03–12.5
c	3x Rushton (3Rt)	0.25–1.75*	1.06–2.12	100–400	20–80	15360–61400	147 408–589 633	0.03–12.5

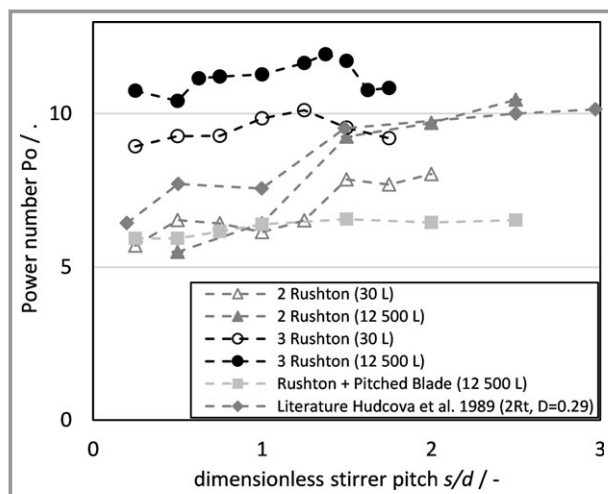


Figure 4. Experimentally determined power numbers Po and comparison with Hudcova et al. [35].

is introduced, which is the ratio between the respective power number Po_i and the power number $Po_{Rt,i}$ for a single Rushton turbine in each system. The normalized Po_{norm} is plotted in Fig. 5. For Figs. 4 and 5 the maximum error is less than 1.3 % of the mean value and is, therefore, not shown.

It can be stated that for the normalized Po_{norm} , the dependency of the stirrer spacing is comparable for both the lab- and industrial-scale reactor as well as with Hudcova et al. [35] for a two-stage Rushton setup. However, compared to the industrial scale the normalized Po_{norm} is recognizably higher for this setup with dimensionless stirrer pitch values less than one in the 30-L scale and literature. Furthermore, on industrial scale, there is no significant influence on the power input for a dimensionless stirrer pitch smaller than one between the two-stage Rushton and the Rushton/pitched blade (RtPb) setup. This is particularly interesting since a single Rushton turbine has a much higher

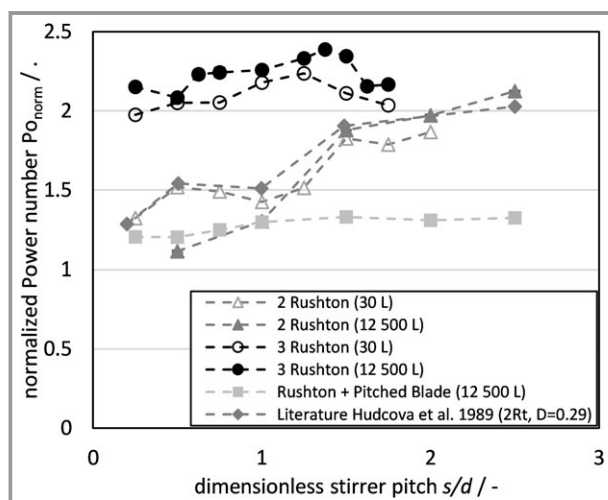


Figure 5. Normalized power numbers Po_{norm} and comparison with Hudcova et al. [35].

power number compared to a single pitched blade. Furthermore, the maximal power number of the three-stage Rushton setup is not significantly higher than the power number of the two-stage Rushton setup. However, the maximal power number has been determined at a dimensionless stirrer pitch of $s/d = 1.5$ for the three-stage Rushton setup.

In the second part of this work, the influence of aeration on the power input for the given stirrer setups will be shown. Therefore, the deviation of the power number under aeration compared to the unaerated system is plotted over the dimensionless stirrer pitch for each setup in Fig. 6. The plotted values are measured at the highest stirrer Reynolds number $Re_{stirrer} = 6.6 \cdot 10^5$. It can be concluded that aeration will, as expected, lead to a decrease of the power number. Furthermore, the aerated power number will decrease slightly more at higher dimensionless stirrer pitches for the two-stage Rushton and RtPb setup (Fig. 6a and 6b). In addition, for the three-stage Rushton setup the effect of aeration on the power number for small and high dimensionless stirrer pitches is less compared to the two-stage stirrer setups (see Fig. 6d). However, aeration will lead to a much higher decrease of the power number for a symmetric distribution ($s/d \approx 1$) of the three Rushton turbines (Fig. 6c at $s/d \approx 1$). This is thought of as being based on the formation of three segregated compartments [36].

Due to these, the stirrers will load the middle compartment with gas, leading to a drop in local density of the multiphase and, thereby, to a drop in the power input. In case of an unsymmetrical distribution of the three stirrers the resulting middle compartment is less loaded with gas. This is of particular importance because a symmetrical distribution of the stirrers is generally preferred. Additionally, a symmetrical distribution of the stirrers does not have the highest possible power number and will lead to a significantly worsened power input performance under aeration as well. Therefore, this effect should be taken into account when scale-up is based on mixing time and mass transfer performance, which both are sensitive to power input.

In the last part of the evaluation, the experimentally determined effect of aeration on the power number will be compared with correlations available from the literature. Therefore, the measured values for Po_G/Po_0 are plotted over the calculated values for the RtPb and three-stage Rushton configuration in Fig. 7. As a correlation parameter the gas flow number Fl_G is used. As already shown in Fig. 6, the spacing of the RtPb configuration in the industrial-scale reactor has less effect on the power number. Furthermore, the measured data are in good agreement with the predicted data for the three-stage Rushton and RtPb configuration in the 30-L reactor. Whereas, the measured influence of aeration in the industrial scale is much smaller than predicted by Calderbank [22]. One possible explanation for this is that the ratio of bubble diameter to stirrer diameter is much larger for the lab-scale reactor than for the industrial-scale reactor. Therefore, the aerated power number Po_G of the industrial-scale reactor is less influenced by aeration than

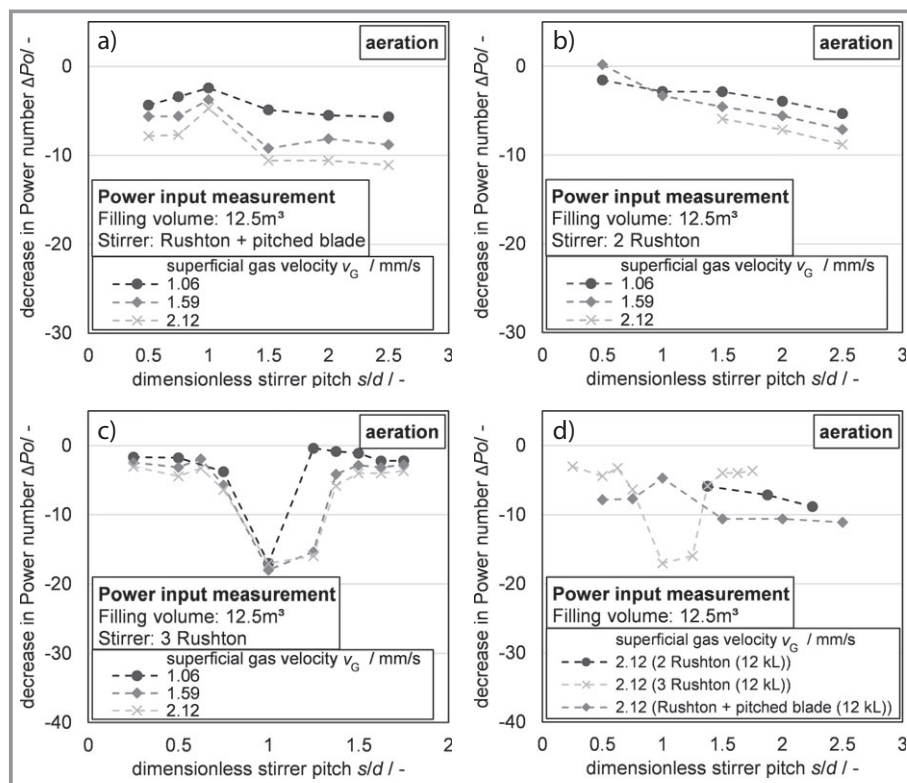


Figure 6. Experimentally determined power numbers for different superficial gas velocities v_G normalized to the unaerated power number for each stirrer setup (a–c) and comparison of the influence of the highest superficial gas velocity v_G on the power number between the stirrer setups (d).

the lab-scale reactor at same gas flow numbers Fl_G . Furthermore, the coherent turbulent structures introduced by the stirrer will scale with the reactor geometry whereas the isotropic turbulence will scale with the specific power input P/V . Thus, the ratio between the coherent turbulent structures and the isotropic turbulence cannot be kept constant during scale-up. This makes the predictive scale-up even more difficult.

5 Conclusion

The objective of this work was to investigate the influence of stirrer spacings for different stirrer types on the mechanical power input characteristics of an aerated stirred tank reactor. Therefore, power input measurements have been performed at a 30- and 12 500-L scale and have been compared with available data from literature. The results from experiments indicate good consistency to the data from Hudcova et al. [35] for the two-stage stirrer combination. However, the influence of small stirrer spacing ($s/d < 1$) for the industrial reactor is significantly smaller than for the 30-L reactor and the data from Hudcova et al. [35]. In addition, the highest power number was determined for the three-stage Rushton combinations with an asymmetrical distribution of the agitators of $s/d = 1.5$.

In case of aeration, the power number will decrease by up to 10 % for the two-stage stirrer combination and large spacings, whereas a drop in the power number by up to

18 % for the three-stage Rushton combination was determined. However, a symmetrical distribution of the stirrers does not have the highest possible power number and will lead to a significantly worsened power input performance under aeration as well. Therefore, this effect should be taken into account when scale-up is based on mixing time and mass transfer performance, which both are sensitive to power input.

The authors gratefully thank Boehringer Ingelheim Pharma GmbH & Co. KG for the financial support to conduct the presented research and ZETA Biopharma for the provision of the BMRF bottom-driven magnetic stirrer for the industrial-scale reactor.

Symbols used

a	$[\text{Nm n}^{-2}]$	slope in Eq. (16)
d	$[\text{m}]$	diameter (impeller)
D	$[\text{m}]$	diameter (reactor)
Fl_G	$[-]$	gassed flow number
Fr	$[-]$	Froude number
H	$[\text{m}]$	height
L	$[\text{m}]$	length
M	$[\text{N m}]$	torque
n	$[\text{s}^{-1}]$	stirrer frequency
N	$[-]$	number of stirrers

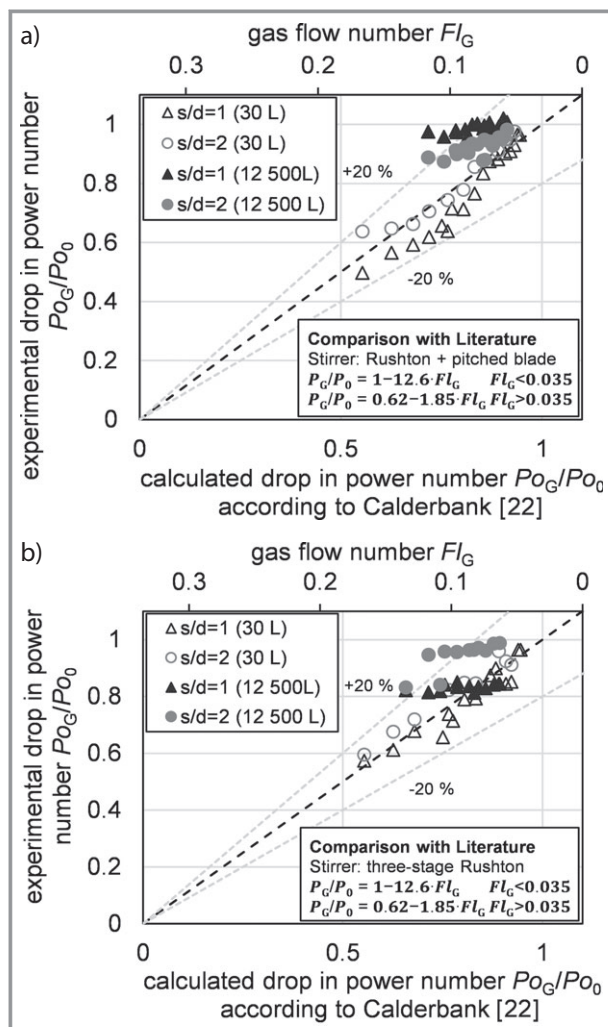


Figure 7. Comparison between the experimentally determined effect of aeration on the power number and the calculated power numbers according to [22] for the 30-L reactor and the 15000-L reactor: Rushton + pitched blade setup (a) and three-stage Rushton (b).

P	[W]	power consumption
P_0	[-]	power number
q	[m ³ s ⁻¹]	impeller pumping capacity
q_G	[m ³ s ⁻¹]	gas flow rate
Re	[-]	Reynolds number
s	[m]	spacing
u_G	[m s ⁻¹]	superficial gas velocity
V	[m ³]	volume
\dot{V}	[m ³ s ⁻¹]	volume flux
w	[m]	impeller width

Greek letters

ε_G	[-]	gas hold-up
η	[Pa s]	dynamic viscosity

ρ	[kg m ⁻³]	density
σ	[mN m ⁻¹]	fluid surface tension

Sub- and Superscripts

B	baffle
stirrer	stirrer
G	gas
G	aerated condition
i	30-L or 12 000-L scale
L	liquid
R	reactor
stat	stationary
0	unaerated condition

References

- J. C. Middleton, L. M. Smith, *Handbook of Industrial Mixing* (Eds: E. L. Paul, V. A. Atiemo-Obeng, S. M. Kresta), John Wiley & Sons, Hoboken, NJ 2003.
- F. Garcia-Ochoa, E. Gomez, *Biotech. Adv.* **2009**, *27*, 153–176. DOI: <https://doi.org/10.1016/j.biotechadv.2008.10.006>
- M. Zlokarnik, *Scale-up: Modellübertragung in der Verfahrenstechnik*, 2th ed. Wiley-VCH, Weinheim 2005.
- H.-J. Henzler, *Chem. Ing. Tech.* **2007**, *79* (7), 951–965. DOI: <https://doi.org/10.1002/cite.200600112>
- P. Zehner, in *Mischen und Rührer: Grundlagen und moderne Verfahren* (Ed: M. Kraume), Wiley-VCH, Weinheim 2003.
- M. Zlokarnik, *Chem. Ing. Tech.* **1967**, *39* (9–10), 539–548. DOI: <https://doi.org/10.1002/cite.330390909>
- M. Warmoeskerken, J. M. Smith, *Chem. Eng. Sci.* **1985**, *40* (11), 2063–2071. DOI: [https://doi.org/10.1016/0009-2509\(85\)87023-8](https://doi.org/10.1016/0009-2509(85)87023-8)
- V. C. Haß, A. W. Nienow, *Chem. Ing. Tech.* **1989**, *61* (2), 152–154. DOI: <https://doi.org/10.1002/cite.330610213>
- A. W. Nienow, *Appl. Mech. Rev.* **1998**, *51* (1), 3–32. DOI: <https://doi.org/10.1115/1.3098990>
- M. Bouaifi, G. Hebrard, D. Bastoul, M. Roustan, *Chem. Eng. Process.* **2001**, *40* (2), 97–111. DOI: [https://doi.org/10.1016/S0255-2701\(00\)00129-X](https://doi.org/10.1016/S0255-2701(00)00129-X)
- L. N. Kong, W. Li, L.-C. Han, Y.-J. Liu, H.-A. Luo, M. Al Dahhan, M. P. Dudukovic, *Chem. Eng. J.* **2012**, *188*, 191–198. DOI: <https://doi.org/10.1016/j.cej.2012.02.023>
- G. Montante, D. Horn, A. Paglianti, *Chem. Eng. Sci.* **2008**, *63* (8), 2107–2118. DOI: <https://doi.org/10.1016/j.ces.2008.01.005>
- M. Laakkonen, M. Honkanen, P. Saarenrinne, J. Aittamaa, *Chem. Eng. J.* **2005**, *109* (1–3), 37–47. DOI: <https://doi.org/10.1016/j.cej.2005.03.002>
- A. Busciglio, F. Grisafi, F. Scargiali, A. Brucato, *Chem. Eng. Sci.* **2013**, *102*, 551–566. DOI: <https://doi.org/10.1016/j.ces.2013.08.029>
- B. W. Lee, M. P. Dudukovic, *Chem. Eng. Sci.* **2014**, *109*, 264–275. DOI: <https://doi.org/10.1016/j.ces.2014.01.032>
- Z. Chara, B. Kysela, J. Konfrst, I. Fort, *Appl. Math. Comput.* **2016**, *272*, 614–628. DOI: <https://doi.org/10.1016/j.amc.2015.06.044>
- G. Montante, A. Paglianti, F. Magelli, *Chem. Eng. Res. Des.* **2007**, *85* (5), 647–653. DOI: <https://doi.org/10.1205/cherd06141>
- A. Rosseburg, J. Fitschen, J. Wutz, T. Wucherpennig, M. Schlüter, *Chem. Eng. Sci.* **2018**, *188*, 208–220. DOI: <https://doi.org/10.1016/j.ces.2018.05.008>



SPECIFYING GAS TRANSFER

www.zeta.com/kLa



verbesserte
Produktqualität & -reinheit,
höhere Produktausbeute,
gesteigerte
Prozesssicherheit

- [19] R. Eibl, D. Eibl, R. Pörtner, G. Catapano, P. Czermak, *Cell and Tissue Reaction Engineering*, Springer-Verlag, Heidelberg **2009**.
- [20] H. Chmiel, *Bioprozesstechnik*, 3rd ed., Springer Spektrum, Heidelberg **2011**.
- [21] M. Bouaifi, M. Roustan, *Chem. Eng. Process.* **2000**, 40 (2), 87–95. DOI: [https://doi.org/10.1016/S0255-2701\(00\)00128-8](https://doi.org/10.1016/S0255-2701(00)00128-8)
- [22] P.-H. Calderbank, *Trans. Inst. Chem. Eng.* **1958**, 36, 443–463.
- [23] S. Nagata, *Mixing: Principles and Applications*, Halstead Press, New York **1975**.
- [24] H. T. Luong, B. Volesky, *AIChE J.* **1979**, 25, 893–895.
- [25] M. Reuss, R. K. Bajpai, K. Lenze, *Scale-up strategies based on the interactions of transport and reaction*, 6th International Fermentation Symposium, London, Ontario, Canada, **1980**.
- [26] G. A. Hughmark, *Ind. Eng. Chem. Process Des. Dev.* **1980**, 19, 638–641.
- [27] *Fermentation and Biochemical Engineering Handbook* (Eds: H. C. Vogel, C. M. Todaro), 2nd ed., William Andrew, Waltham, MA **1996**.
- [28] O. B.-J. Platas Barradas, *Process and Cultivation Strategies for the Human Industrial Cell Line AGE1.HN.*, Ph.D. Thesis, Technische Universität Hamburg **2014**.
- [29] S.-J. Wang, J.-J. Zhong, *Biotech. Bioeng.* **1996**, 51, 520–527. DOI: [https://doi.org/10.1002/\(SICI\)1097-0290\(19960905\)51:5<520::AID-BIT3>3.0.CO;2-E](https://doi.org/10.1002/(SICI)1097-0290(19960905)51:5<520::AID-BIT3>3.0.CO;2-E)
- [30] J. Markopoulos, E. Babalona, E. Tsiliopoulou, *Chem. Eng. Technol.* **2004**, 27 (11), 1212–1215. DOI: <https://doi.org/10.1002/ceat.200402129>
- [31] J. Markopoulos, E. Babalona, E. Tsiliopoulou, K. Tasopoulou, *Chem. Eng. Technol.* **2005**, 28 (9), 978–981. DOI: <https://doi.org/doi.org/10.1002/ceat.200500172>
- [32] S. Tiam You, A. A. A. Raman, R. S. S. R. E. Shah, M. I. M. Nor, *Rev. Chem. Eng.* **2014**, 30 (3), 323–336. DOI: <https://doi.org/10.1515/revce-2013-0028>
- [33] V. W. Uhl, J. B. Gray, *Mixing*, Vol. 1, Academic Press, New York **1966**.
- [34] E. Babalona, D. Bahouma, S. Tagia, E. Pantouflas, J. Markopoulos, *Chem. Eng. Technol.* **2005**, 28 (7), 802–807. DOI: <https://doi.org/10.1002/ceat.200407160>
- [35] V. Hudcova, V. Machon, A. W. Nienow, *Biotechnol. Bioeng.* **1989**, 34, 617–628. DOI: <https://doi.org/10.1002/bit.260340506>
- [36] X. Minghui, X. Jianye, Y. Zhen, C. Ju, Z. Yingpin, Z. Siliang, *Ind. Eng. Chem. Res.* **2014**, 53, 5941–5953. DOI: <https://doi.org/10.1021/ie400831s>
- [37] R. Davis, *Design and Scale-Up of Production Scale Stirred Tank Fermentors*, Master of Science, Utah State University **2009**.